ELSEVIER

Polymer 40 (1999) 5249–5255

polymer

Development of bicontinuous morphologies in polysulfone–epoxy blends

P.A. Oyanguren, M.J. Galante, K. Andromaque[1], P.M. Frontini, R.J.J. Williams*

Institute of Materials Science and Technology (INTEMA), University of Mar del Plata and National Research Council (CONICET), J. B. Justo 4302, (7600) Mar del Plata, Argentina

Received 25 May 1998; accepted 8 October 1998

Abstract

The development of bicontinuous morphologies in 10 wt% polysulfone (PSu)–epoxy (DGEBA)/anhydride (MTHPA) blends, was followed by optical and scanning electron microscopy. Blends cured at 80°C revealed the formation of large epoxy-rich domains surrounded by a PSu-rich matrix, soon after the cloud point. Advancing the cure led to an increase in the volume fraction and the coalescence of epoxy-rich domains. A bicontinuous primary morphology was thus generated. A secondary phase separation was observed in both primary phases from the very beginning of the phase-separation process. While spinodal demixing was clearly the mechanism by which the primary morphology was generated, nucleation-growth could be responsible of the secondary phase separation. Postcure steps produced a change in the composition of phases as revealed by DMA, and in the secondary morphology as observed by SEM. A postcure at 120°C led to a single T_g at 115°C with a small shoulder at higher temperatures. A postcure at 200°C led to a T_g at 108°C for the epoxy-rich phase and a T_g at 137°C for the PSu-rich phase. The partial purification of the thermoplastic phase produced a significant enhancement of toughness. K_{IC} was increased from 0.65 MPa $m^{1/2}$ for the neat thermoset to 1.10 MPa $m^{1/2}$ for the blend postcured at 200°C.

Keywords: Polysulfone–epoxy blends; Thermoplastic-modified epoxies; Epoxy-anhydride networks

1. Introduction

A large number of studies on thermoset (TS)/thermoplastic (TP) blends have been published in recent years. Several engineering thermoplastics associated with different thermosetting polymers have been investigated. Polysulfone (PSu)-modified epoxies have been the subject of several of these studies [1–14]. PSu is initially soluble in the precursors of the thermosetting polymer but a phase separation process takes place in the course of polymerization leading to materials exhibiting an increase in fracture toughness. Thermodynamic analysis of the reaction-induced phase separation in modified thermosets [13–22], provides an explanation of the morphologies generated under different cure conditions.

Morphologies generated in TS/TP blends depend on the location of the initial TP concentration with respect to the critical composition. Off-critical compositions in the range of low TP concentrations give place to a dispersion of TP domains in a TS matrix. Off-critical compositions in the range of high TP concentrations lead to phase-inverted structures consisting of a dispersion of TS domains in a TP matrix. This range of compositions is the one used for the processing of intractable polymers like poly(2,6-dimethyl-1,4 phenylene ether) (PPE), using reactive solvents [23–25]. Compositions located close to the critical point give place to bicontinuous and related morphologies, which are usually desired to obtain a significant increase in toughness [26].

We have recently analyzed the phase separation induced by a chain polymerization for the particular case of a polysulfone-modified epoxy/anhydride system [14]. Formulations containing 10 wt% PSu became phase-separated at very low conversions (cloud-point conversion, $x_{cp} = 0.10$), leading to bicontinuous morphologies. On account of the low viscosity of the solution at the time of phase separation, generated structures had large dimensions, i.e. in the range where optical microscopy may be employed to follow the development of morphologies.

The aim of this paper will be the analysis of the formation of bicontinuous structures in a PSu–epoxy/anhydride blend by using optical and scanning electron microscopy. The influence of postcure steps on morphologies generated and

* Corresponding author.

[1] On leave from Laboratoire des Matériaux Macromoléculaires, UMR CNRS N° 5627, INSA de Lyon, 20 Av. Albert Einstein, 69621 Villeurbanne Cedex, France.

0032-3861/99/$ - see front matter
PII: S0032-3861(98)00742-3

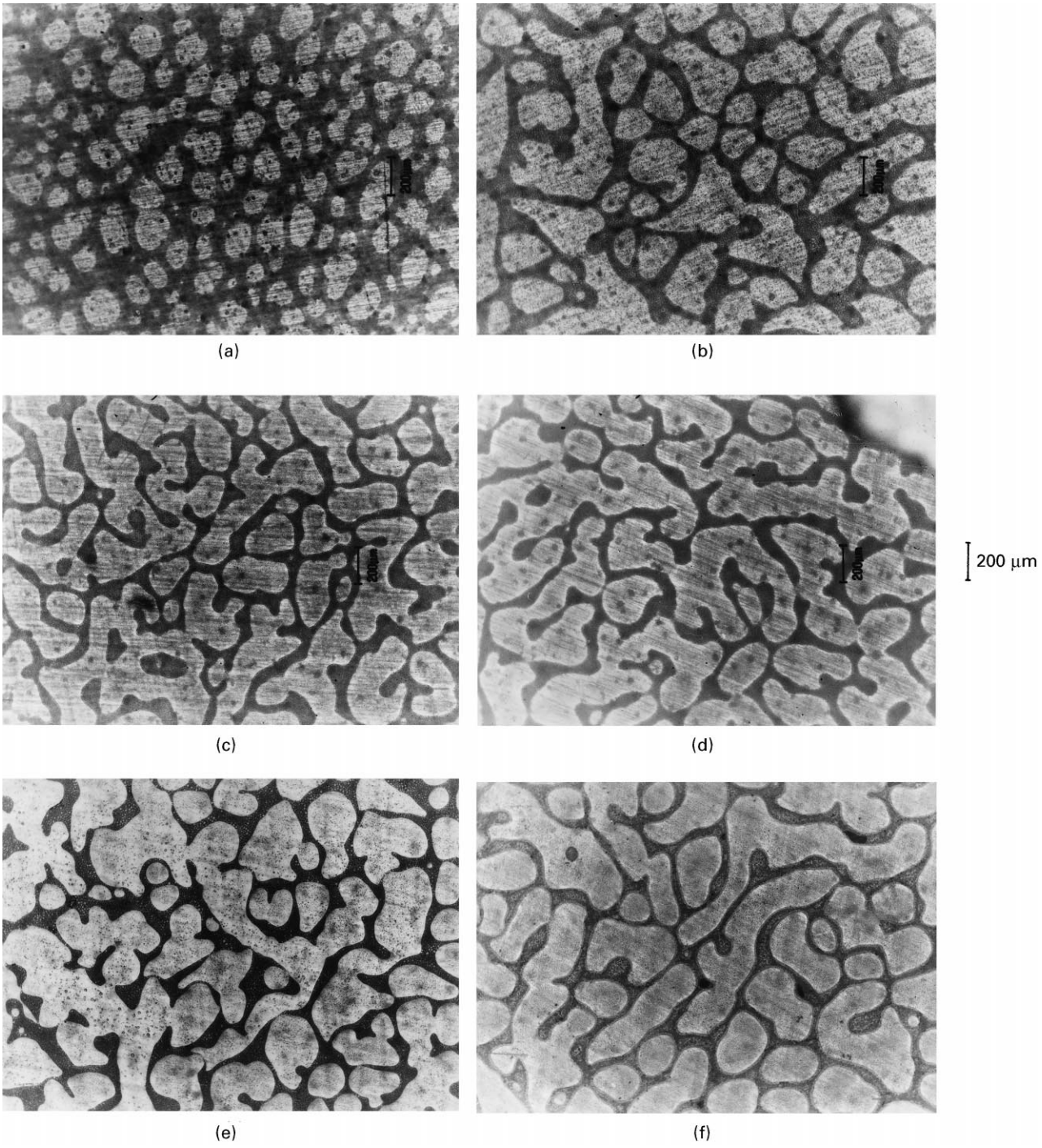

Fig. 1. Development of morphologies in a 10 wt% PSu–epoxy/anhydride blend cured at 80°C, followed by optical microscopy. (a) 30 min, (b) 40 min, (c) 60 min, (d) 90 min, (e) after a postcure at 120°C, (f) after a postcure at 200°C.

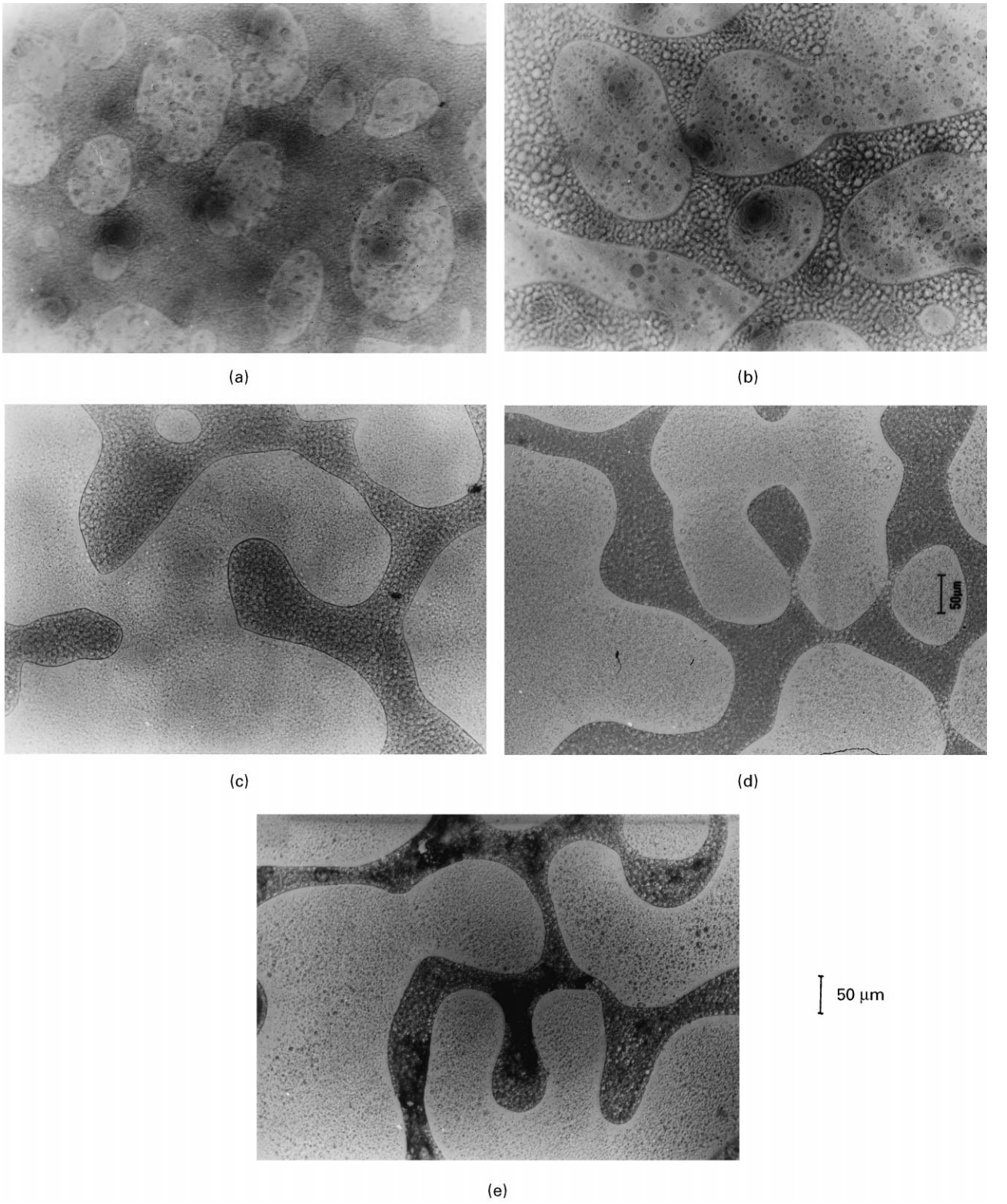

Fig. 2. Optical micrographs with higher magnification for the same system shown in Fig. 1. (a) 30 min, (b) 40 min, (c) 60 min, (d) after a postcure at 120°C, (e) after a postcure at 200°C.

on the fracture resistance of resulting materials will be discussed.

2. Experimental

2.1. Materials and preparation of samples

An epoxy resin based on diglycidylether of bisphenol A (DGEBA, MY 790 Ciba-Geigy), was used. It had a weight per epoxy group, WPE = 173.8 g mol^{-1}, as determined by acid titration, and was dried under vacuum at 80°C before use. The anhydride was methyl tetrahydrophthalic anhydride (MTHPA, HY 918 Ciba-Geigy), used in stoichiometric proportion, i.e. anhydride groups/epoxy groups = 1. The initiator was benzyldimethylamine (BDMA, Sigma), used in a molar ratio with respect to epoxy groups, i_0/e_0 = 0.043. The thermoplastic modifier was a commercial-grade polysulfone (PSu, Amoco Chemicals, Udel P1700).

Initial solutions were prepared as follows. DGEBA and the amount of PSu required to get a 10 wt% in the final material, were dissolved in methylene chloride. Most of the solvent was evaporated at room temperature and the residual amount was eliminated by heating at 80°C for 24 h. The anhydride was incorporated during the cooling stage to room temperature, i.e. at about 50°C. Finally, the initiator was added at room temperature. A clear homogeneous solution was obtained.

2.2. Optical microscopy (OM)

A drop of the mixture was placed between glass slides held together with clamps. A set of these samples was cured in an oven at 80°C. Partially cured specimens were extracted at different times for observation with an Olympus Inverted Microscope PMG3. The influence of postcure steps carried out at 120°C for 2 h or at 200°C for 1 h, was analyzed.

2.3. Mechanical characterization

Plaques for subsequent mechanical characterization were obtained by casting the mixture into a mold consisting of two glass plates coated with siliconized paper and spaced by rubber cords of 3 mm diameter, for dynamic mechanical analysis, and 6 mm diameter, for fracture tests. Cure was carried out in an oven at T = 80°C for 4 h. Postcure was performed either at 120°C for 2 h or at 200°C for 1 h.

Dynamic mechanical spectra were obtained with a Perkin-Elmer DMA-7 system, operating at 1 Hz in the three-point-bending mode, using a 10°C/min heating rate. Specimens with dimensions of 20 mm × 3 mm × 2 mm (thickness), were machined from the plaques.

Fracture test specimens were obtained using a diamond saw. Central V-shaped notches were machined in the bars followed by gently tapping a razor blade into the notch so as to grow a natural crack ahead of the razor blade ($0.45 < a/W < 0.55$, where a is the total crack length and W is the width of the specimen). The span to width (S/W) and the thickness to width (B/W) ratios were kept equal to 4 and 0.5, respectively. The fracture test was carried out at room temperature in an Instron 4467 Universal Testing Machine, operated in the three-point-bending mode at a crosshead displacement rate of 10 mm/min. The stress intensity factor at the onset of crack growth, K_{IC}, was calculated following the European Protocol [27]. The total crack length (a) was measured from the fracture surface using a profile projector with a magnification of 10. In the case of thermoplastic-modified materials, the crack length was evidenced by the use of a red penetrant ink.

Fracture surfaces were coated with a fine gold layer and observed by scanning electron microscopy (JEOL JSM 35 CF).

3. Results and discussion

Fig. 1 shows the development of the bicontinuous structure in the 10 wt% PSu–epoxy/anhydride blend cured at 80°C, followed by optical microscopy. The overall picture is characteristic of spinodal demixing. Dark areas correspond to a PSu-rich phase while clear domains indicate an epoxy-rich phase. The assignment is based on the behavior of these phases in a fracture test, as revealed by SEM micrographs, and is confirmed by the analytical identification of phases in a similar system [10].

The cloud-point time was t_{cp} = 28 min, corresponding to a cloud-point conversion, x_{cp} = 0.10 [14]. The first micrograph with enough contrast between phases was recorded 2 min after the beginning of phase separation (Fig. 1a). A droplet-type morphology composed of epoxy-rich domains of average size in the order of 10^2 μm, surrounded by a PSu-rich matrix, is observed. This type of morphology may be originated by an initial bicontinuous structure undergoing a very fast percolation-to-cluster transition [28,29]. As the cure proceeds, the volume fraction of the epoxy-rich phase increases because of the continuous segregation of epoxy-anhydride species from the PSu-rich phase. This leads to coalescence of epoxy-rich domains and the generation of a bicontinuous structure.

The thermosetting polymer gels at t_{gel} = 58 min (x_{gel} = 0.44) [14]. From this time on, the primary morphology (the one observed at this magnification) is quenched as shown by Figs. 1c,d (taken at t = 60 min and at t = 90 min, respectively). Vitrification of PSu-rich domains may be expected to occur at 80°C giving a phase containing a significant concentration of monomers and low-molar-mass oligomers of the thermosetting polymer [14] (the glass transition temperature of the neat PSu is 190°C). These species will remain trapped in the glassy domains and will come again into reaction during the postcure steps. Figs. 1e,f show the morphologies resulting from postcure steps at 120°C and 200°C, respectively. No major changes with respect to

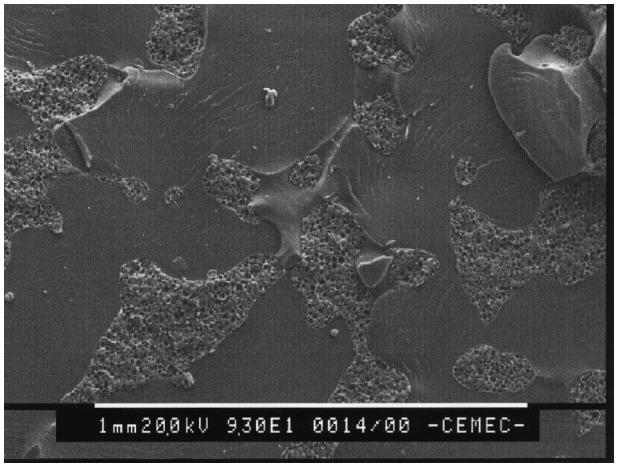

Fig. 3. SEM micrograph after a postcure at 120°C.

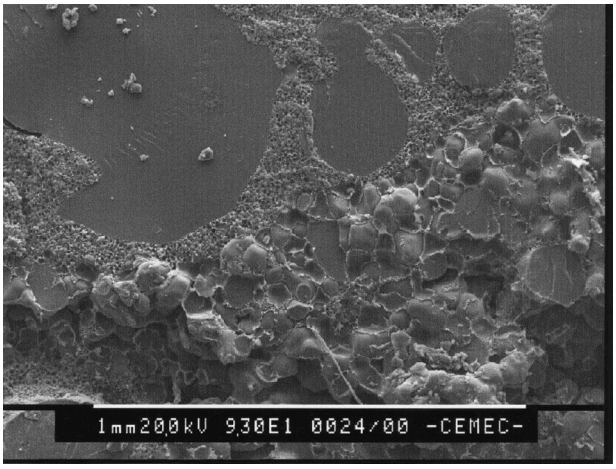

Fig. 5. SEM micrograph after a postcure at 200°C.

morphologies already generated in the pregel stage at 80°C, were observed at this magnification.

Fig. 2 shows optical micrographs at a higher magnification. A secondary phase separation occurring in both phases from the early stages of structure development, is evidenced. This morphology is usually referred to as phase-in-phase morphology or double-phase morphology. Epoxy-rich domains exhibit a dispersion of PSu-rich particles that were phase-separated from the thermosetting polymer as conversion increased. These particles did not coalesce with the continuous thermoplastic-rich phase. Similarly, epoxy-rich particles were segregated from the PSu-rich phase. These domains did not coalesce with the continuous thermosetting phase possibly as a result of the high viscosity of the thermoplastic-rich phase.

Although spinodal demixing is clearly the mechanism by which the primary morphology is generated, it is indeed possible that a nucleation-growth mechanism be responsible of the secondary phase separation in both phases. This possibility has been suggested in the literature [19].

The influence of postcure steps on morphology was followed by SEM of fracture surfaces. Secondary morphologies resulting from a postcure step at 120°C (Figs. 3 and 4) show differences from those derived from the postcure step at 200°C (Figs. 5 and 6). At 200°C, the maximum T_g of any of both phases is exceeded so that the maximum possible conversion and purification of phases will result. After a postcure at 120°C, a unimodal distribution of the epoxy-rich particles (average size of about 10 μm), dispersed in the thermoplastic-rich phase, is observed. After a postcure at 200°C, a bimodal distribution with average sizes of the order of about 5 and 50 μm, is evidenced. This is the result of the devitrification of the PSu-rich phase with a continuation of the TS polymerization and a redistribution of species between both phases.

Dynamic mechanical analysis gives a better picture of the influence of a postcure step. As observed in Fig. 7, the postcure at 120°C leads to a major relaxation peak at 115°C, with a small shoulder at higher temperatures. The existence of two phases cannot be clearly discerned from

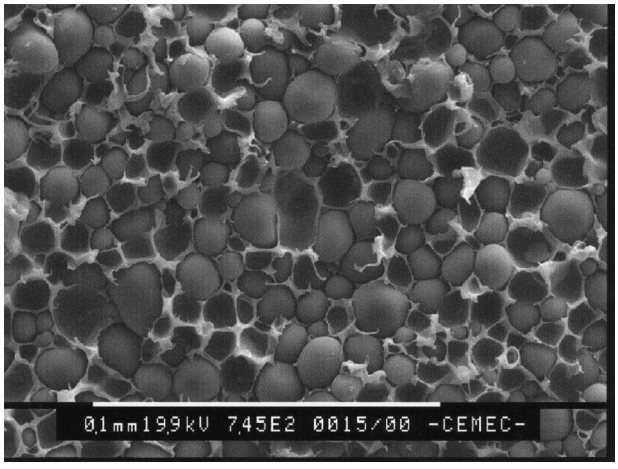

Fig. 4. SEM micrograph after a postcure at 120°C (higher magnification).

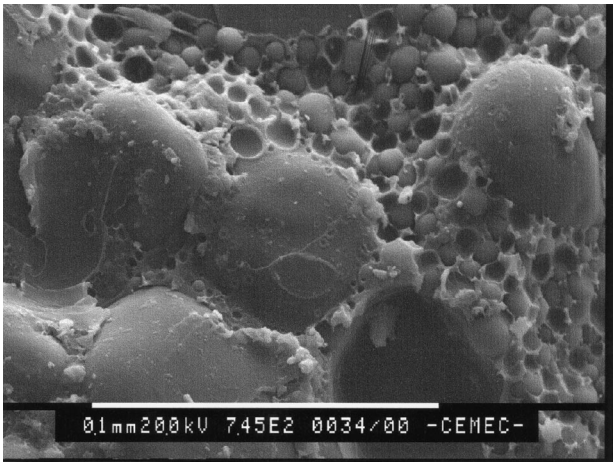

Fig. 6. SEM micrograph after a postcure at 200°C (higher magnification).

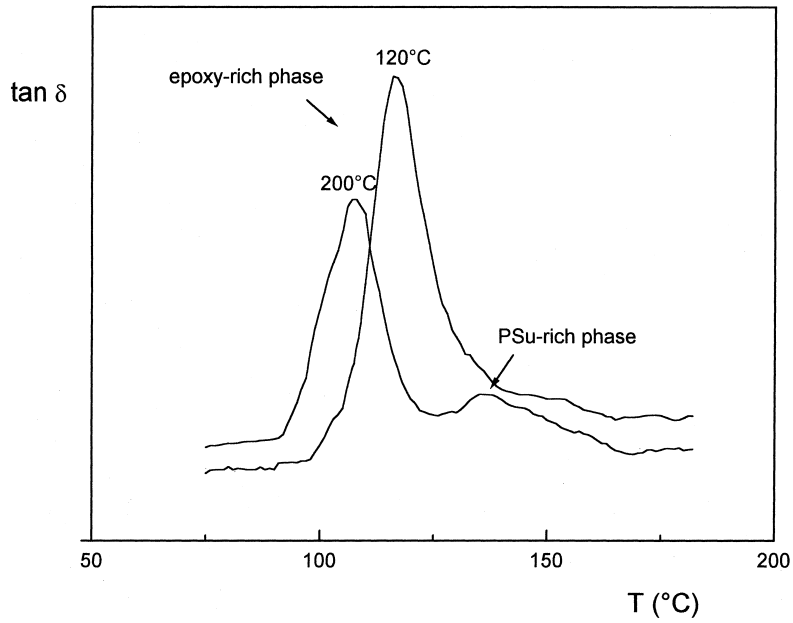

Fig. 7. Tan δ versus temperature for 10 wt% PSu–epoxy anhydride blends postcured at 120°C and 200°C.

this thermogram. The postcure at 200°C enables one to identify the presence of an epoxy-rich phase ($T_g = 108$°C) and a PSu-rich phase ($T_g = 137$°C). This means that the TP-rich phase has segregated a fraction of the epoxy-anhydride species, a fact that caused a decrease of the TS-T_g and an increase of the TP-T_g. However, the T_g value of neat PSu (about 190°C), is not attained.

The fracture resistance of the cured blends showed a significant dependence of the selected postcure cycle. K_{IC} values were 0.65 MPa $m^{1/2}$ for the neat thermoset, 0.80 MPa $m^{1/2}$ for the blend postcured at 120°C and 1.10 MPa $m^{1/2}$ for the blend postcured at 200°C. The large increase in fracture toughness produced by the postcure at high temperatures is probably related to the partial purification of the PSu-rich phase as revealed by the increase in its glass transition temperature. Analysis of SEM micrographs put in evidence the following toughening mechanisms: (a) in the TS-rich phase, crack-path deflection, bifurcation lines and plastic drawing of PSu-rich particles; (b) in the TP-rich phase, plastic drawing of the PSu-rich phase together with signs of stress whitening and debonding of TS-rich particles. The simultaneous presence of all these toughening mechanisms explains the significant increase of the fracture resistance.

In order to have a better evaluation of the mechanical performance of the materials one has to take into account that the phase separation into large phases also generates the presence of large defects. This means that although K_{IC} values may be high, other mechanical parameters like the yield stress in tension or the strain at failure may be severely deteriorated with respect to the neat epoxy. For example, specimens of the PSu-modified epoxy tested in compression exhibited an aleatorious behavior after the yield point. While some specimens could be compressed to large strains, other ones failed rapidly after the maximum load. Therefore, although the generation of large domains proved to be useful to get an understanding of the phase separation mechanism through the use of optical microscopy, the resulting structures led to the deterioration of the overall mechanical properties.

4. Conclusions

The development of bicontinuous morphologies in 10 wt% PSu–epoxy/anhydride blends, could be followed by optical microscopy because of the large characteristic size of the domains generated. Soon after the cloud-point, a droplet-type morphology consisting of epoxy-rich domains of average size in the order of 10^2 μm, surrounded by a PSu-rich matrix, was observed. As the cure proceeded, an increase in the volume fraction and coalescence of the epoxy-rich domains was produced, because of the partial segregation of the thermosetting polymer from the thermoplastic-rich phase. A bicontinuous primary morphology was thus generated, with characteristic features practically arrested at gelation of the thermoset. The overall picture of primary morphology generation was characteristic of a spinodal demixing mechanism.

A secondary phase separation was observed in both phases starting soon after the cloud point. PSu-rich particles were segregated in the TS-rich phase while TS-rich particles were generated in the PSu-rich phase, leading to a double-phase bicontinuous morphology. The generation of the secondary morphology (dispersed-phase particles) was considered typical of a nucleation-growth process although no direct evidence of this assumption was provided.

Postcure steps produced a change in the composition of

both phases as revealed by DMA, and in the secondary morphology as observed by SEM. A postcure step at 120°C led to a unimodal distribution of TS-rich particles in the TP-rich phase. A single T_g was observed, with a small shoulder at higher temperatures. A postcure step at 200°C led to a bimodal distribution of TS-rich particles and a clear identification of the T_gs of both phases, i.e. T_g = 108°C for the TS-rich phase and 137°C for the PSu-rich phase. Blends postcured at 200°C exhibited a significant increase in the fracture resistance. The critical stress intensity factor increased from K_{IC} = 0.65 MPa $m^{1/2}$ for the neat thermoset to 1.10 MPa $m^{1/2}$ for the PSu-modified material.

Acknowledgements

The financial support of CONICET (PIP 4070/96) and Fundación Antorchas (Argentina), is gratefully acknowledged.

References

[1] Hedrick JL, Yilgor Y, Wilkes GL, McGrath JE. Polym Bull 1985;13:201.
[2] Cecere JA, McGrath JE. Polym Prepr Am Chem Soc Div Polym Chem 1986;27:299.
[3] Jabloner H, Swetlin BJ, Chu SG. US Patent 4,656,207 (1987).
[4] Chu SG, Swetlin BJ, Jabloner H. US Pat. 4,656,208 (1987).
[5] Fu Z, Sun Y. Polym Prepr Am Chem Soc Div Polym Chem 1988;29:177.
[6] Hedrick JL, Yilgor I, Jurek M, Hedrick JC, Wilkes GL, McGrath JE. Polymer 1991;32:2020.
[7] MacKinnon AJ, Jenkins SD, McGrail PT, Pethrick RA. Polymer 1993;34:3252.
[8] Min BG, Stachurski ZH, Hodgkin JH. J Appl Polym Sci 1993;50:1511.
[9] MacKinnon AJ, Pethrick RA, Jenkins SD, McGrail PT. Polymer 1994;35:5319.
[10] Woo EM, Bravenec LD, Seferis JC. Polym Eng Sci 1994;34:1664.
[11] de Graaf LA, Hempenius MA, Möller M. Polym Prepr Am Chem Soc Div Polym Chem 1995;36:787.
[12] Varley RJ, Hodgkin JH, Hawthorne DG, Simon GP. J Polym Sci Part B: Polym Phys 1997;35:153.
[13] Elliniadis S, Higgins JS, Clarke N, McLeish TCB, Choudhery RA, Jenkins SD. Polymer 1997;38:4855.
[14] Oyanguren PA, Riccardi CC, Williams RJJ, Mondragon I. J Polym Sci Part B: Polym Phys 1998;36:1349.
[15] Williams RJJ, Borrajo J, Adabbo HE, Rojas AJ. Rubber-modified thermoset resins. In: Riew CK, Gillham JK, editors. Adv Chem Ser, 208. Washington, DC: American Chemical Society, 1984:195.
[16] Vazquez A, Rojas AJ, Adabbo HE, Borrajo J, Williams RJJ. Polymer 1987;28:1156.
[17] Moschiar SM, Riccardi CC, Williams RJJ, Verchère D, Sautereau H, Pascault HJP. J Appl Polym Sci 1991;42:717.
[18] Riccardi CC, Borrajo J, Williams RJJ. Polymer 1994;35:5541.
[19] Clarke N, McLeish TCB, Jenkins SD. Macromolecules 1995;28:4650.
[20] Borrajo J, Riccardi CC, Williams RJJ, Cao ZQ, Pascault JP. Polymer 1995;36:3541.
[21] Riccardi CC, Borrajo J, Williams RJJ, Girard-Reydet E, Sautereau H, Pascault JP. J Polym Sci B Polym Phys 1996;34:349.
[22] Williams RJJ, Rozenberg BA, Pascault JP. Adv Polym Sci 1997;128:95.
[23] Venderbosch RW, Meijer HEH, Lemstra PJ. Polymer 1994; 35:4349.
[24] Venderbosch RW, Meijer HEH, Lemstra PJ. Polymer 1995;36:1167.
[25] Venderbosch RW, Meijer HEH, Lemstra PJ. Polymer 1995;36:2903.
[26] Kinloch AJ, Yuen ML, Jenkins SD. J Mater Sci 1994;29:3781.
[27] Williams JG, Cawood MJ. Polymer Testing 1990;9:15.
[28] Binder K. Solid State Commun 1980;34:191.
[29] Barton BF, Graham PD, McHugh AJ. Macromolecules 1998; 31:1672.